# EXPERIMENTAL INVESTIGATION AND DIRECT STRENGTH DESIGN OF HIGH STRENGTH COMPLEX C-SECTIONS IN PURE BENDING

CAO HUNG PHAM
GREGORY J. HANCOCK

RESEARCH REPORT R925
JANUARY 2012

ISSN 1833-2781

SCHOOL OF CIVIL ENGINEERING

THE UNIVERSITY OF SYDNEY

THE UNIVERSITY OF SYDNEY

SCHOOL OF CIVIL ENGINEERING

# EXPERIMENTAL INVESTIGATION AND DIRECT STRENGTH DESIGN OF HIGH STRENGTH COMPLEX C-SECTIONS IN PURE BENDING

**RESEARCH REPORT R925**

**CAO HUNG PHAM**
**GREGORY J. HANCOCK**

February 2012

ISSN 1833-2781

ISSN 1833-2781



Published by:
School of Civil Engineering
The University of Sydney
Sydney NSW 2006
Australia

This report and other Research Reports published by the School of Civil Engineering are available at http://sydney.edu.au/civil

## ABSTRACT

Plain C or Z-sections are two of the most common cold-formed steel shapes in use throughout the world. Other shapes are high strength SupaCee® and SupaZed® steel sections which are widely used in Australia as purlins in roof and wall systems. They contain additional return lips and web stiffeners which enhance the bending capacity of the sections. Design methods for these sections are normally specified in the Australian/New Zealand Standard for Cold-Formed Steel Structures (AS/NZS 4600:2005) or the North American Specification for Cold-Formed Steel Structural Members (NAS S100-2007). In both Standards, which include the newly developed Direct Strength Method of design (DSM), the method presented (Chapter 7 of AS/NZS 4600:2005, Appendix 1 of NAS) is developed for beams and columns, including the reliability of the method. This report presents two different test series on both plain C- and SupaCee® sections in pure bending. They were performed at the University of Sydney for the extension of the DSM to include channel section beams with complex stiffeners. Two different section depths and three different thicknesses of high strength lipped channel sections were tested in pure bending. Tests with and without torsion/distortion restraint straps screwed on the top flanges in the pure bending region were also considered to allow local and distortional buckling to form in the sections respectively. Test results and formulae developed from the DSM are summarized in the report. Three different cases where moments are used in association with yield, inelastic or plastic criteria in the DSM local and distortional strength equations are compared with the test data. By comparisons between cases, a proposed recommendation for DSM inelastic buckling strength design in pure bending with extended non-dimensional slenderness limit for both local and distortional buckling is given in the report.

## KEYWORDS

Cold-formed steel; Complex channel sections; High strength steel; Direct strength method; Pure bending test; Inelastic buckling strength; Plastic moment.

## TABLE OF CONTENTS

## INTRODUCTION

Roof systems composed of high tensile steel profiled sheeting screw-fastened to cold formed steel purlins of high strength steel are widely used in civil construction. Two of the most common purlins employed in these applications are the C- and Z-sections. In Australia, the new SupaCee® and SupaZed® steel purlin profiles developed by Bluescope Lysaght (Lysaght, 2003) and the University of Sydney give higher capacities and more economical solutions. The longitudinal web stiffeners and return lip stiffeners of these sections significantly improve the performance when bending capacity governs. Currently, two basic design methods for cold-formed steel members are formally available in the Australian/New Zealand Standard for Cold-Formed Steel Structures (AS/NZS 4600:2005) (Standards Australia, 2005) or the North American Specification for Cold-Formed Steel Structural Members (NAS, S100-2007). They are the traditional Effective Width Method (EWM) and the newly developed Direct Strength Method of design (DSM) (Chapter 7 of AS/NZS 4600:2005, Appendix 1 of NAS S100-2007). As sections become more complex with additional multiple longitudinal web stiffeners and return lips as designed on SupaCee® and SupaZed® sections, the computation of the effective widths becomes more complex. For the EWM, the calculation of effective widths of the numerous sub-elements leads to severe complications with decreased accuracy. In some special cases, no design approach is even available for such a section using the EWM. The DSM appears to be more beneficial and simpler by using the elastic buckling stresses of the whole sections such as the SupaCee® and SupaZed®. There is no need to calculate cumbersome effective sections especially with intermediate stiffeners.

In the development of the DSM, Yu and Schafer conducted two series of flexural tests and finite element analyses on a variety of C- and Z-Sections with local buckling (Yu and Schafer, 2003) and distortional buckling (Yu and Schafer, 2006). Those series aimed at isolating the local and distortional modes used in verifying the DSM. Recently, additional tests on distortional buckling have also been conducted by Javaroni and Goncalves (2006). The main purpose of this report is to provide additional experimental data on channel sections in pure bending performed at the University of Sydney. Both plain C- and SupaCee® sections were tested in the four point bending arrangement. Two different depths and three different thicknesses of each type of channels were tested in the above series. Half of the tests were conducted with straps attached on the top flanges in the pure bending region by self-tapping screws. The straps allowed the channels to buckle in local buckling modes. The remaining tests were tested without those straps on the top flanges which allowed distortional buckling failures. The current DSM is based on the yield moment $(M_y)$ of the sections. However, a recent proposal by Shifferaw and Schafer (2007) allows an inelastic moment $(M_n)$ to be used. Another alternative is the plastic moment $(M_p)$. The test results are plotted against the DSM local and distortional curves for beams where the three cases associated with yield $(M_y)$, inelastic $(M_n)$ and plastic $(M_p)$ moments are used for comparison. Based on the comparisons of test results with these cases, this report recommends a new proposal for DSM design in pure bending to extend the non-dimensional slenderness limit for the inelastic moment determination to more slender sections for both local and distortional buckling. Calibration of all cases outlined in Chapter F in the North American Specification (AISI, 2007) is included in this report.

## EXPERIMENTAL INVESTIGATIONS ON PLAIN C- AND SUPACEE® SECTIONS IN PURE BENDING

### TEST RIG DESIGN

The experimental program comprised a total of twenty four tests (12 for plain lipped C- sections and 12 for SupaCee® sections) conducted in the J. W. Roderick Laboratory for Materials and Structures at the University of Sydney. All tests were performed in the 2000 kN capacity DARTEC testing machine, using a servo-controlled hydraulic ram. A diagram of the test set-up and overview test photo for the common four point loading configuration is shown in Fig. 1. The channel section members were tested in pairs with flanges facing inwards and with a gap between them to ensure inside assembly was possible.

At the supports, the two beam specimens were bolted through the webs by vertical rows of M12 high tensile bolts. These rows of bolts were connected to two channel sections 250x90x6CC with stiffeners. Steel plates of 20 mm thickness were used as load transfer plates which were also bolted through the flanges of the channel sections 250x90x6CC with stiffeners. These load bearing plates rested on the half rounds of the DARTEC supports to simulate a set of simple supports.

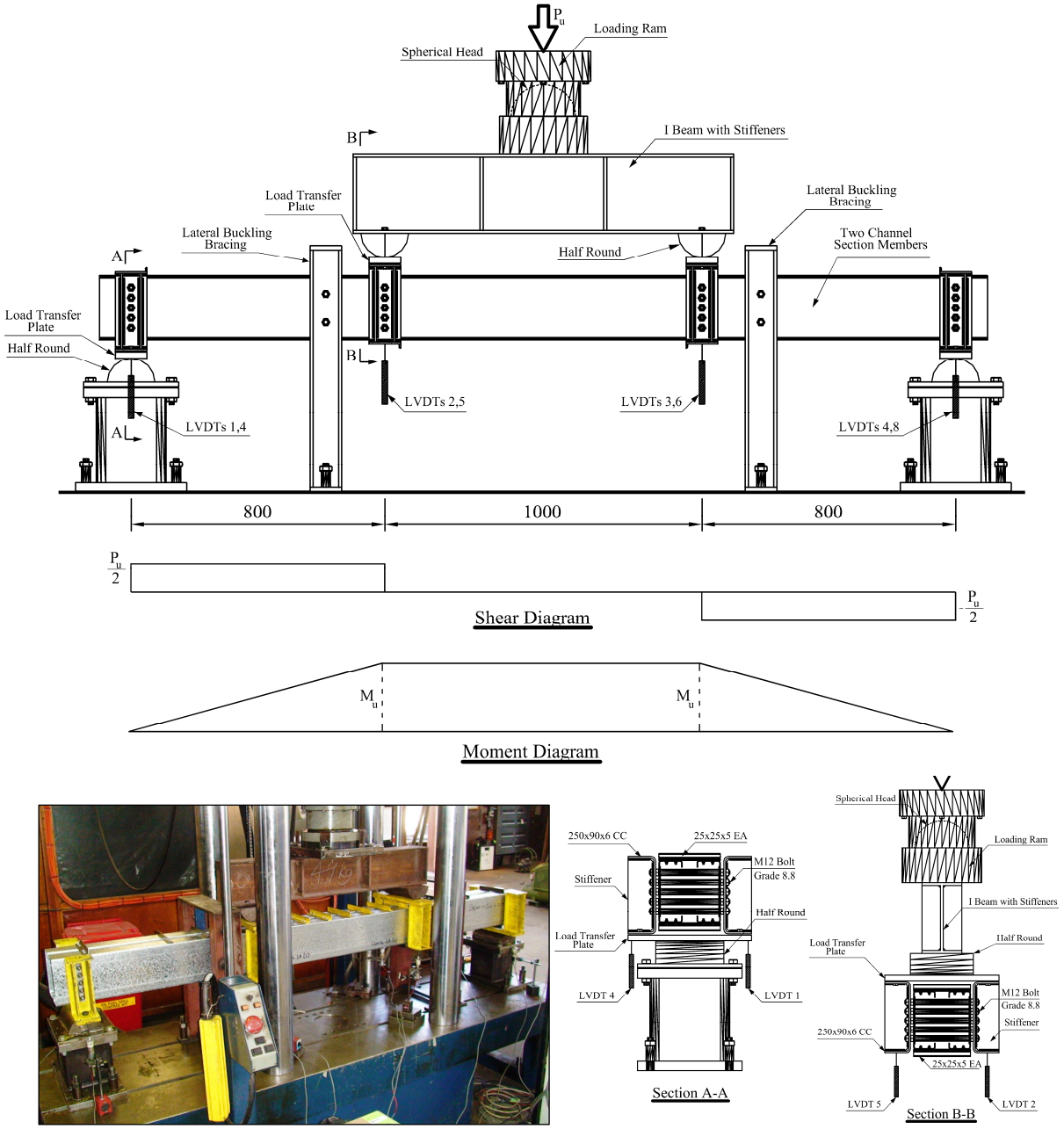


Figure 1. Pure Bending Test Set-up Configuration-Actual Experimental Test (200mm Depth Section)

At the loading point at mid-span, the DARTEC loading ram has a spherical head to ensure that the load is applied uniformly, and moved downwards at a constant stroke rate of 2 mm/min during testing. The load was transferred to the channel section members via a centrally loaded spreader I beam which had two half rounds at two ends. The distance between the two half rounds was 1000 mm. These two half rounds bore upon two 20 mm thick load transfer plates. The half rounds ensured that the applied loads were vertical. The load was then transferred to two channel sections 250x90x6CC with stiffeners which were connected to the test beam specimens by two vertical rows of M12 high tensile bolts. Four and five rows of bolts were used at each support and loading point for the 150mm and 200mm depth sections respectively. The distance between the support and the adjacent loading point was 800 mm. Eight LVDTs (Linear Variable Displacement Transducers) were utilized for the pure bending test series as shown in Fig. 1. All LVDTs were mounted directly to the base of the DARTEC testing machine. This set-up allowed for the vertical displacement of the specimen to be determined without being affected by bending of the test specimen. To prevent flexural-torsional buckling, two lateral buckling braces as also shown in Fig.1 were installed to ensure that all tests failed due to local or distortional buckling.

## TESTS WITH STRAPS (LOCAL BUCKLING) AND WITHOUT STRAPS (DISTORTIONAL BUCKLING)

For the pure bending test series, twelve tests (6 for plain lipped C- sections and 6 for SupaCee® sections) were tested with eight 25x25x5EA straps which were uniformly distributed in the pure bending moment region between the two loading points as shown in Fig. 2(a). The purpose of the straps is to force the channel members to buckle locally rather than by distortional buckling. The other twelve remaining tests (6 for plain C-lipped sections and 6 for SupaCee® sections) in this series were tested without the six middle 25x25x5EA straps as shown in Fig. 2(b). Only two straps adjacent to the loading points were attached to the channel members to prevent distortion at the loading points.

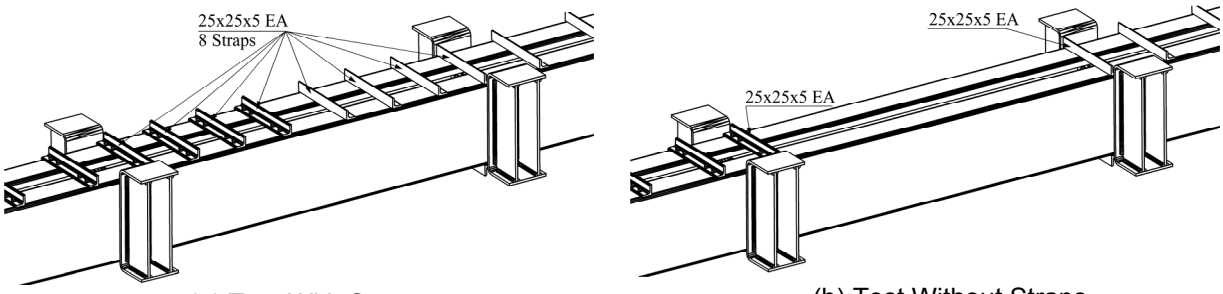


(a) Test With Straps (b) Test Without Straps

Figure 2. Tests With Straps (Local Buckling) and Without Straps (Distortional Buckling)

## SPECIMEN NOMENCLATURE, DIMENSIONS AND COUPON TEST RESULTS

The test specimens were labeled in order to express the pure bending series, tests with or without straps, channel section, depth and thickness. Typical test labels for plain C- "Ms-C15015" and SupaCee® sections "Mw-SC15015" are defined as follows:

- M indicates the pure bending test series. "s" indicates the test with straps and a "w" expresses the test "without" straps attached in the pure bending region.
- "C150" and "SC150" indicate plain C- section (C150) and SupaCee® section (SC150) respectively with the web depth of 150 (alternatively "C200" and "SC200").
- The final "15" is the actual thickness (1.5 in mm) times 10 (alternatively "12", "19" and "24").

Two different commercially available plain lipped C- and SupaCee® sections of 150 and 200 mm depths were chosen with three different thicknesses of 1.5, 1.9 and 2.4 mm (for plain lipped C- sections) and 1.2, 1.5 and 2.4 mm (for SupaCee® sections). The average measured dimensions for the pure bending test series are shown in Fig. 3 and in Table 1 respectively.

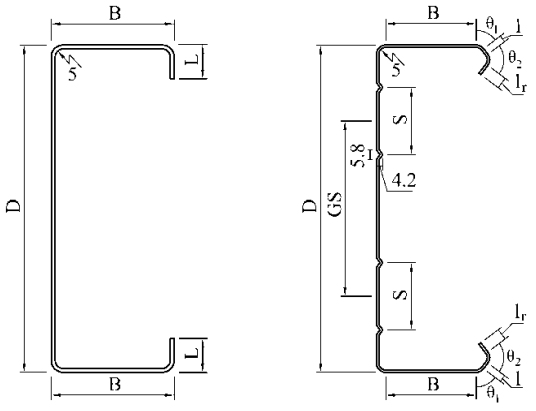


Figure 3. Dimensions of Plain C- and SupaCee® Channel Sections

Thirty six coupons (18 for plain lipped C- sections and 18 for SupaCee® sections) were taken longitudinally from the compression flange flat, the tension flange flat and the centre of the web flat of each channel section member. The tensile coupon dimensions conformed to the Australian Standard AS 1391 (Standards Australia 1991) for the tensile testing of metals using 12.5 mm wide coupons with gauge length 50 mm. The test specimens were galvanized by two layers of corrosion protection coating during the manufacturing process. Since the thickness of the steel sheet is very thin, these coatings may allow the steel to carry more load, hence the base metal thickness of the virgin material had to be determined. The coatings were removed to expose the virgin (base) material by acid etching. The total thickness of the two coatings is 0.05 mm. The tests were performed using the 300 kN capacity Sintech/MTS 65/G testing machine operated in a displacement control mode. The mean value of the coupon test for each specimen size and thickness is shown in Appendices 1 and 2 for plain lipped C- sections and SupaCee® sections respectively. The yield stress $f_y$ was obtained by using the 0.2 % nominal proof stress and was also included in Table 1.

| Test | Section | Thickness (mm) | D (mm) | B (mm) | L (mm) | l (mm) | lr (mm) | GS (mm) | S (mm) | $\theta_1$ ($^0$) | $\theta_2$ ($^0$) | $f_y$ (MPa) |
|---|---|---|---|---|---|---|---|---|---|---|---|---|
| Ms | C15015 | 1.5 | 153.46 | 64.53 | 15.02 | - | - | - | - | - | - | 541.13 |
| Ms | C15019 | 1.9 | 153.54 | 65.01 | 16.27 | - | - | - | - | - | - | 534.48 |
| Ms | C15024 | 2.4 | 153.43 | 63.58 | 20.88 | - | - | - | - | - | - | 485.29 |
| Ms | C20015 | 1.5 | 203.74 | 75.88 | 16.16 | - | - | - | - | - | - | 513.40 |
| Ms | C20019 | 1.9 | 203.53 | 79.27 | 17.51 | - | - | - | - | - | - | 510.48 |
| Ms | C20024 | 2.4 | 202.30 | 77.58 | 21.26 | - | - | - | - | - | - | 483.49 |
| Ms | SC15012 | 1.2 | 153.68 | 42.31 | - | 5.78 | 6.35 | 63.84 | 40.37 | 53.5 | 83.5 | 589.71 |
| Ms | SC15015 | 1.5 | 152.61 | 42.85 | - | 4.75 | 5.91 | 63.53 | 41.31 | 55.5 | 82.5 | 533.88 |
| Ms | SC15024 | 2.4 | 153.75 | 44.57 | - | 4.84 | 5.25 | 60.89 | 42.32 | 51.5 | 82.5 | 513.68 |
| Ms | SC20012 | 1.2 | 205.37 | 54.57 | - | 6.92 | 6.29 | 109.39 | 42.36 | 56.0 | 83.0 | 593.30 |
| Ms | SC20015 | 1.5 | 203.99 | 54.36 | - | 7.01 | 6.72 | 109.56 | 42.17 | 57.0 | 85.0 | 532.03 |
| Ms | SC20024 | 2.4 | 203.21 | 54.63 | - | 6.79 | 8.36 | 110.34 | 41.54 | 55.5 | 85.5 | 504.99 |
| Mw | C15015 | 1.5 | 152.70 | 64.77 | 16.51 | - | - | - | - | - | - | 541.13 |
| Mw | C15019 | 1.9 | 153.38 | 64.47 | 16.00 | - | - | - | - | - | - | 534.48 |
| Mw | C15024 | 2.4 | 152.60 | 62.70 | 19.70 | - | - | - | - | - | - | 485.29 |
| Mw | C20015 | 1.5 | 203.70 | 76.08 | 16.42 | - | - | - | - | - | - | 513.40 |
| Mw | C20019 | 1.9 | 202.60 | 77.92 | 17.28 | - | - | - | - | - | - | 510.48 |
| Mw | C20024 | 2.4 | 203.35 | 76.61 | 20.88 | - | - | - | - | - | - | 483.49 |
| Mw | SC15012 | 1.2 | 153.78 | 43.02 | - | 5.41 | 6.03 | 63.39 | 40.75 | 55.0 | 86.0 | 589.71 |
| Mw | SC15015 | 1.5 | 153.47 | 42.82 | - | 4.97 | 6.93 | 64.68 | 41.64 | 56.5 | 83.5 | 533.88 |
| Mw | SC15024 | 2.4 | 153.88 | 43.95 | - | 5.43 | 5.71 | 60.53 | 42.55 | 53.0 | 84.0 | 513.68 |
| Mw | SC20012 | 1.2 | 205.65 | 54.35 | - | 6.36 | 7.09 | 109.44 | 42.51 | 56.5 | 85.0 | 593.30 |
| Mw | SC20015 | 1.5 | 203.91 | 54.05 | - | 7.18 | 6.95 | 109.49 | 42.54 | 55.0 | 85.5 | 532.03 |
| Mw | SC20024 | 2.4 | 203.64 | 54.87 | - | 6.87 | 8.41 | 110.51 | 41.74 | 57.0 | 86.5 | 504.99 |
| Internal Radius r = 5 mm | | | | | | | | | | | | |

Table 1. Specimen Dimensions and Properties of Plain C- and SupaCee® Channel Sections

## ELASTIC INSTABILITIES FOR THE CHANNEL CROSS-SECTIONS

Cold-formed thin-walled channel purlins may undergo one of the three modes of local, distortional and lateral-torsional buckling or combinations of these. The Semi-Analytical Finite Strip Method (SAFSM) developed by Cheung (1976) has been widely used in computer software THIN-WALL (CASE, 2006) or CUFSM (Schafer and Ádány, 2006) to develop the signature curve of buckling stress versus buckling half-wavelength for thin-walled sections under compression and bending to allow identification of these modes. Fig. 4 shows a comparison of the signature curves of both the plain lipped C- (C20015) and SupaCee® (SC20015) sections in bending.

As can be seen in Fig. 4, the buckling stresses associated with both the local and distortional buckling modes of SC20015 increase significantly compared with those of C20015 where the areas of these two sections are almost the same. The reason for this fact is due to four additional longitudinal web stiffeners and the return

lips. They enhance the bending capacity of the sections for both local and distortional modes at short and intermediate half-wavelength respectively. Meanwhile, the buckling stresses for the lateral-torsional mode in one half-wave over the unbraced length of the purlins are almost unchanged. The minimum points of these curves are used in the Direct Strength Method (DSM) of design of cold-formed sections. Determination of the bending strength capacity requires consideration of these cross section instabilities, post-buckling characteristics, interaction between modes, and material yielding.

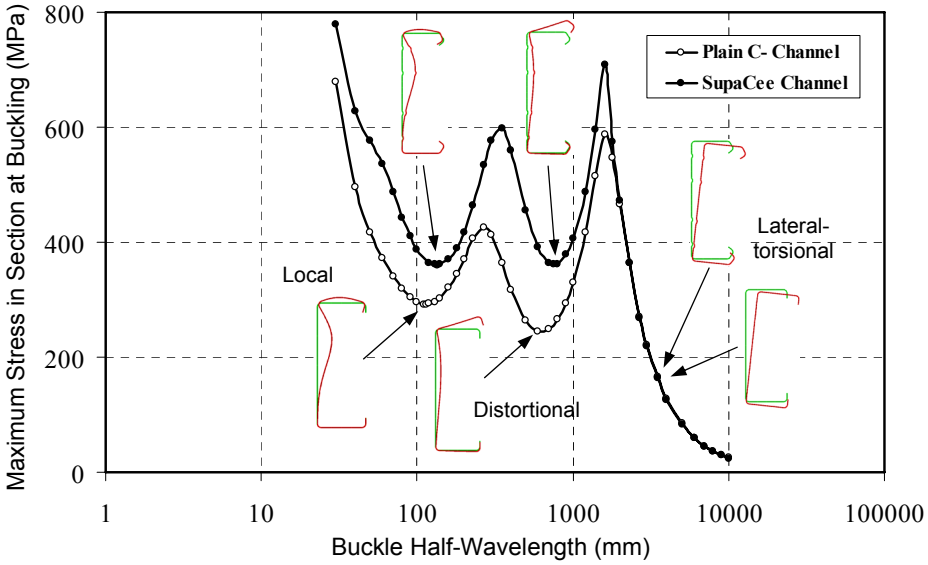


Figure 4. Buckling Modes of Cold-Formed Plain C- and SupaCee® Sections

## DIRECT STRENGTH METHOD (DSM) RULES OF DESIGN FOR FLEXURE

### LOCAL BUCKLING STRENGTH

The nominal section moment capacity at local buckling *($M_{sl}$)* is determined from Section 7.2.2.3 of AS/NZS 4600:2005 [Appendix 1, Section 1.2.2.2 of NAS (2007)] as follows:

$$\text{For } \lambda_l \le 0.776 \ : \ M_{sl} = M_y \tag{1}$$

$$\text{For } \lambda_l > 0.776 \ : \ M_{sl} = \left[1 - 0.15\left(\frac{M_{ol}}{M_y}\right)^{0.4}\right]\left(\frac{M_{ol}}{M_y}\right)^{0.4} M_y \tag{2}$$

where $\lambda_l$ is non-dimensional slenderness used to determine $M_{sl}$; $\lambda_l = \sqrt{M_y / M_{ol}}$ ; $M_y = Z_f f_y$ ,

$M_{ol}$ is elastic local buckling moment of the section; $M_{ol} = Z_f f_{ol}$ ,

$Z_f$ is section modulus about a horizontal axis of the full section,

$f_{ol}$ is elastic local buckling stress of the section in bending.

### DISTORTIONAL BUCKLING STRENGTH

The nominal section moment capacity at distortional buckling *($M_{sd}$)* is determined from Section 7.2.2.4 of AS/NZS 4600:2005 [Appendix 1, Section 1.2.2.3 of NAS (2007)] as follows:

$$\text{For } \lambda_d \le 0.673 \ : \ M_{sd} = M_y \tag{3}$$

$$\text{For } \lambda_d > 0.673 \ : \ M_{sd} = \left[1 - 0.22\left(\frac{M_{od}}{M_y}\right)^{0.5}\right]\left(\frac{M_{od}}{M_y}\right)^{0.5} M_y \tag{4}$$

where $\lambda_d$ is non-dimensional slenderness used to determine $M_{sd}$; $\lambda_d = \sqrt{M_y / M_{od}}$ ; $M_y = Z_f f_y$ ,
$M_{od}$ is elastic distortional buckling moment of the section; $M_{od} = Z_f f_{od}$ ,
$Z_f$ is section modulus about a horizontal axis of the full section,
$f_{od}$ is elastic distortional buckling stress of the section in bending.

### INELASTIC BUCKLING STRENGTH

Although cold-formed thin-walled steel sections may fail due to numerous cross-section buckling modes, they still may develop inelastic reserve capacity. Shifferaw and Schafer (2007) provided and verified a general method for prediction of inelastic bending capacity of cold-formed steel members. The methodology was based on an extensive experimental data base and nonlinear finite element models. The design approach for the inelastic lateral-torsional buckling is provided based on the hot-rolled steel AISC Specification. The resulting relationships for inelastic local and distortional buckling are provided in a DSM format for adoption in the AISI Specifications as follows:

For $\lambda_l \le 0.776$ and $\lambda_d \le 0.673$, and sections symmetric about the axis of bending:

$$M_n = M_y + \left(1 - 1/C_y^2\right)\left(M_P - M_y\right) \tag{5}$$

where $\lambda_l = \sqrt{M_y / M_{ol}}$ , $\lambda_d = \sqrt{M_y / M_{od}}$ , $C_{yl} = \sqrt{0.776 / \lambda_l} \le 3$ , $C_{yd} = \sqrt{0.673 / \lambda_d} \le 3$

$M_y$ is yield moment, $M_p$ is plastic moment equal to $S_f f_y$ where $S_f$ is the plastic section modulus of the full section.

## TEST RESULTS

Table 2 provides a summary of the 24 four-point bending tests which consist of 12 local buckling tests with straps and 12 distortional tests without straps for both plain C- and SupaCee® sections. Included in Table 2 are the ultimate peak loads *($P_u$)* and the test bending moments *($M_T$)* in the pure bending region of each beam specimen. The elastic local buckling stress *($f_{ol}$)*, the distortional buckling stress *($f_{od}$)*, the elastic section modulus *($Z_f$)* about a horizontal axis of the full section in bending as obtained from computer software THIN-WALL (CASE, 2006) and the plastic section modulus *($S_f$)* are also included. Table 2 is then partitioned into the elastic local buckling moment *($M_{ol}$)*, the elastic distortional buckling moment *($M_{od}$)*, the moment to cause the first yield in each channel based on tension coupon test results *($M_y$)*, the inelastic bending moment *($M_n$)*, the plastic moment *($M_p$)* and the proposed inelastic bending moment *($M_{ny}$)* with extended slenderness limit range of each channel section. The interpretation of the proposed inelastic bending moment *($M_{ny}$)* will be discussed in detail in the following section.

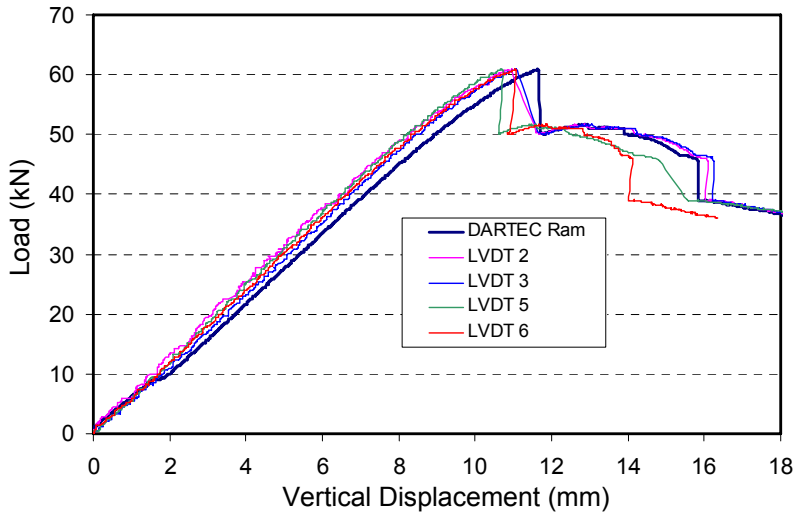


Figure 5. Load-Vertical Displacement Curves of DARTEC Ram and LVDTs for Mw-C20015 Test

Fig. 5 shows a typical load-vertical displacement response of the Mw-C20015 distortional test without straps where all readings from DARTEC ram and LVDTs 2,3,5 and 6 were recorded. Figs. 6(a) and 6(b) show the corresponding local and distortional buckling mode shapes of plain C-members (C20015) with and without straps.

| Test | Section | $P_u$ (kN) | $M_T = V_T \times 0.8$ (kNm) | $f_{ol}$ (MPa) | $f_{od}$ (MPa) | $Z_f$ ($mm^3$) | $S_f$ ($mm^3$) | $M_{ol}$ (kNm) | $M_{od}$ (kNm) | $M_y$ (kNm) | $M_n$ (kNm) | $M_p$ (kNm) | $M_{ny}$ (kNm) |
|---|---|---|---|---|---|---|---|---|---|---|---|---|---|
| Ms | C15015 | 52.13 | 10.43 | 479.3 | 340.3 | 21640 | 24812 | 10.37 | 7.36 | 11.71 | 11.71 | 13.43 | 12.25 |
| Ms | C15019 | 79.30 | 15.86 | 755.7 | 471.7 | 27500 | 31559 | 20.78 | 12.97 | 14.70 | 14.70 | 16.87 | 15.69 |
| Ms | C15024 | 99.19 | 19.84 | 1226 | 772.0 | 34700 | 40088 | 42.54 | 26.79 | 16.84 | 17.33 | 19.45 | 18.39 |
| Ms | C20015 | 67.33 | 13.47 | 292.1 | 243.8 | 35220 | 40687 | 10.29 | 8.59 | 18.08 | 18.08 | 20.89 | 18.49 |
| Ms | C20019 | 108.78 | 21.76 | 454.1 | 321.6 | 45830 | 52774 | 20.81 | 14.74 | 23.40 | 23.40 | 26.94 | 24.52 |
| Ms | C20024 | 156.94 | 31.39 | 741.9 | 509.6 | 57200 | 66100 | 42.44 | 29.15 | 27.66 | 27.66 | 31.96 | 29.72 |
| Ms | SC15012 | 40.96 | 8.19 | 454.6 | 403.9 | 16690 | 19629 | 7.59 | 6.74 | 9.84 | 9.84 | 11.58 | 10.30 |
| Ms | SC15015 | 57.01 | 11.40 | 642.8 | 506.0 | 20610 | 24605 | 13.25 | 10.43 | 11.00 | 11.00 | 13.14 | 11.88 |
| Ms | SC15024 | 105.97 | 21.19 | 1366 | 799.7 | 33810 | 42634 | 46.18 | 27.04 | 17.37 | 18.32 | 21.90 | 20.11 |
| Ms | SC20012 | 53.53 | 10.71 | 246.5 | 271.9 | 27990 | 33015 | 6.90 | 7.61 | 16.61 | 16.61 | 19.59 | 16.60 |
| Ms | SC20015 | 82.41 | 16.48 | 360.4 | 361.0 | 34790 | 41512 | 12.54 | 12.56 | 18.51 | 18.51 | 22.09 | 19.28 |
| Ms | SC20024 | 169.09 | 33.82 | 821.0 | 640.1 | 56060 | 70070 | 46.03 | 35.88 | 28.31 | 28.31 | 35.38 | 31.81 |
| Mw | C15015 | 47.37 | 9.47 | 479.6 | 367.5 | 21770 | 24969 | 10.44 | 8.00 | 11.78 | 11.78 | 13.51 | 12.06 |
| Mw | C15019 | 64.71 | 12.94 | 763.5 | 471.5 | 27260 | 31296 | 20.81 | 12.85 | 14.57 | 14.57 | 16.73 | 15.14 |
| Mw | C15024 | 88.82 | 17.76 | 1252 | 757.2 | 33900 | 39153 | 42.44 | 25.67 | 16.45 | 16.45 | 19.00 | 17.59 |
| Mw | C20015 | 60.98 | 12.20 | 291.8 | 246.3 | 35330 | 40803 | 10.31 | 8.70 | 18.14 | 18.14 | 20.95 | 18.15 |
| Mw | C20019 | 94.25 | 18.85 | 462.7 | 326.8 | 44980 | 51852 | 20.81 | 14.70 | 22.96 | 22.96 | 26.47 | 23.45 |
| Mw | C20024 | 139.42 | 27.88 | 742.9 | 509.9 | 57010 | 65964 | 42.35 | 29.07 | 27.56 | 27.56 | 31.89 | 28.99 |
| Mw | SC15012 | 32.78 | 6.56 | 450.7 | 398.4 | 16800 | 19736 | 7.57 | 6.69 | 9.91 | 9.91 | 11.64 | 10.06 |
| Mw | SC15015 | 50.48 | 10.10 | 640.1 | 528.0 | 20950 | 25052 | 13.41 | 11.06 | 11.18 | 11.18 | 13.37 | 11.71 |
| Mw | SC15024 | 94.19 | 18.84 | 1381 | 835.0 | 33900 | 42800 | 46.82 | 28.31 | 17.41 | 17.41 | 21.99 | 19.21 |
| Mw | SC20012 | 46.33 | 9.27 | 246.2 | 279.0 | 28060 | 33150 | 6.91 | 7.83 | 16.65 | 16.65 | 19.67 | 16.65 |
| Mw | SC20015 | 68.49 | 13.70 | 361.3 | 362.1 | 34740 | 41466 | 12.55 | 12.58 | 18.48 | 18.48 | 22.06 | 18.79 |
| Mw | SC20024 | 145.77 | 29.15 | 817.6 | 644.2 | 56440 | 70509 | 46.15 | 36.36 | 28.50 | 28.50 | 35.61 | 30.76 |

Table 2. Local and Distortional Test Results of Plain C- and SupaCee® Channel Sections

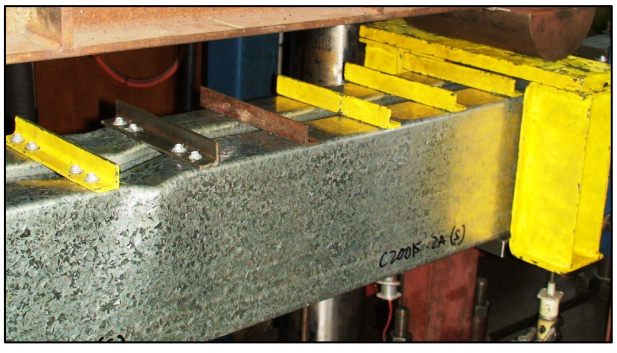

(a) Local Buckling Test with Straps

(b) Distortional Buckling Test without Straps

Figure 6. Local and Distortional Failure Modes of Cold-Formed Plain C-Sections (C20015)

The load-vertical displacement curves for all tests of 150 mm depth sections are graphically reproduced in Fig. 7(a) for the local buckling tests with straps and Fig. 7(b) for the distortional buckling tests without straps. Similarly, Figs 8(a), 8(b) show the load-vertical displacement curves for the local and distortional buckling tests for 200 mm depth sections respectively. As can be seen in Figs 7 and 8, for the very slender sections (e.g., SC15012, SC20012, C20015 and SC20015), the loads increase almost linearly relative to the vertical displacement. The sections failed suddenly in the elastic local and distortional buckling modes. For less slender sections, the load-displacement relationship curves go beyond the linear region and become more nonlinear as they approach the peak loads. Depending on the slenderness of the sections, for the same section depth, the non-linear behaviour is more evident for the thicker sections. For the stocky sections (e.g., C15024 and SC15024), the load-displacement curves almost flatten out prior to the peak loads for both local and distortional buckling tests. Significant nonlinear behaviours for these sections can be particularly observed in Fig. 7a for the local buckling tests (C15024 and SC15024).

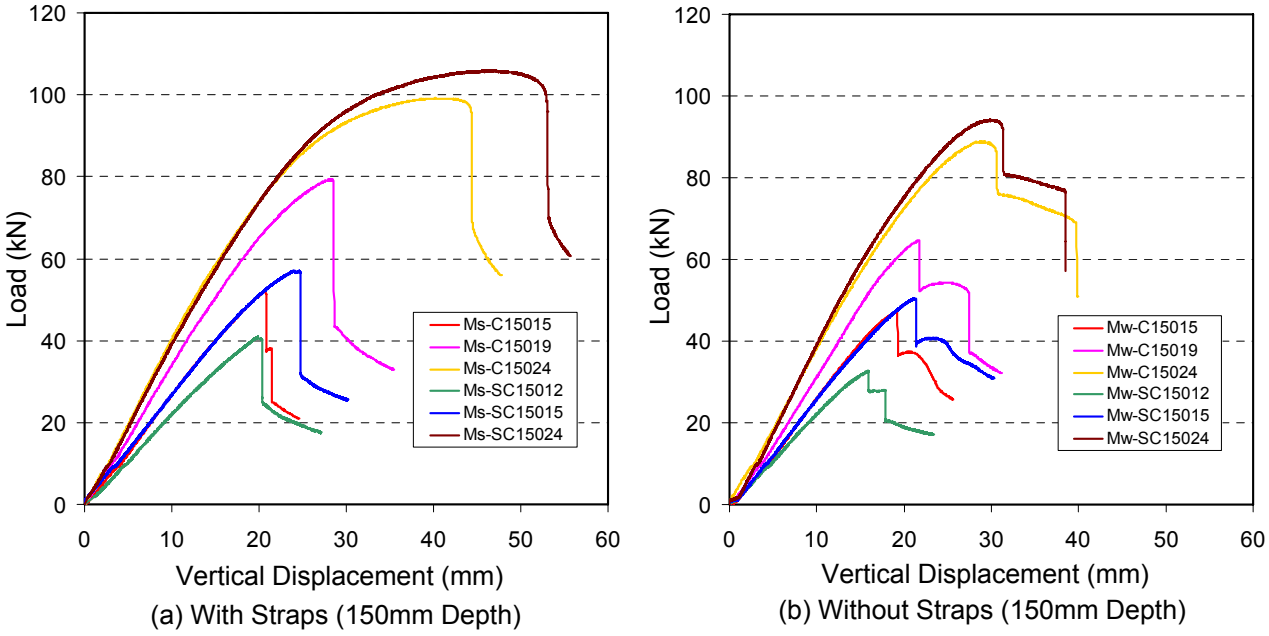


Figure 7. Load-Vertical Displacement Curves of Local and Distortional Buckling tests (150mm Depth Section)

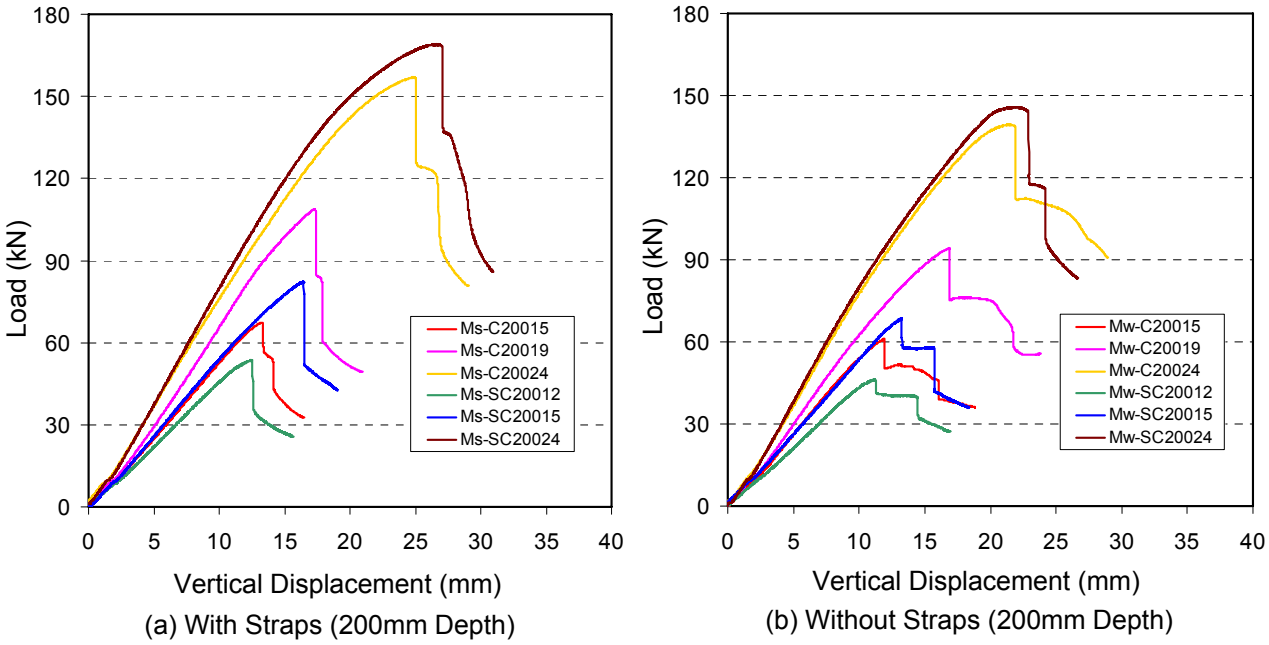


Figure 8. Load-Vertical Displacement Curves of Local and Distortional Buckling tests (200mm Depth Section)

# COMPARISON OF DSM DESIGN LOADS WITH TESTS AND PROPOSAL FOR INELASTIC BUCKLING STRENGTH

## COMPARISON WITH THE EXISTING DSM DESIGN SPECIFICATION

The design models are summarized in Tables 3 and 4 where they are compared with the local and distortional buckling tests respectively. Three different cases namely ***Case A***, ***Case B*** and ***Case C*** where yield *($M_y$)*, inelastic *($M_n$)* and plastic *($M_p$)* moments are used respectively. Based on the comparisons with the test results, ***Case D*** is proposed where the inelastic moment *($M_{ny}$)* is used with an extended slenderness limit range when compared with those used in ***Case B***. The detailed proposals are discussed below. The comparisons with the test data are also provided graphically in Figs. 9(a), 9(b), 9(c) and 9(d) respectively.

| Section | $M_T$ (kNm) | $\lambda_l = \sqrt{\frac{M_y}{M_{ol}}}$ | $\lambda_{lp} = \sqrt{\frac{M_p}{M_{ol}}}$ | $\lambda_{ln} = \sqrt{\frac{M_{ny}}{M_{ol}}}$ | ***Case A*** | | ***Case B*** | | ***Case C*** | | ***Case D*** | |
|---|---|---|---|---|---|---|---|---|---|---|---|---|
| | | | | | $\frac{M_T}{M_y}$ | $\frac{M_T}{M_{sl}}$ | $\frac{M_T}{M_n}$ | $\frac{M_T}{M_{sl}}$ | $\frac{M_T}{M_p}$ | $\frac{M_T}{M_{sl}}$ | $\frac{M_T}{M_{ny}}$ | $\frac{M_T}{M_{sl}}$ |
| C15015 | 10.43 | 1.063 | 1.138 | 1.087 | 0.890 | 1.090 | 0.890 | 1.090 | 0.777 | 0.996 | 0.851 | 1.058 |
| C15019 | 15.86 | 0.841 | 0.901 | 0.869 | 1.079 | 1.135 | 1.079 | 1.135 | 0.940 | 1.033 | 1.011 | 1.085 |
| C15024 | 19.84 | 0.629 | 0.676 | 0.658 | 1.178 | 1.178 | 1.145 | 1.145 | 1.020 | 1.020 | 1.079 | 1.079 |
| C20015 | 13.47 | 1.326 | 1.425 | 1.341 | 0.745 | 1.060 | 0.745 | 1.060 | 0.645 | 0.965 | 0.728 | 1.045 |
| C20019 | 21.76 | 1.060 | 1.138 | 1.085 | 0.930 | 1.137 | 0.930 | 1.137 | 0.808 | 1.035 | 0.887 | 1.102 |
| C20024 | 31.39 | 0.807 | 0.868 | 0.837 | 1.135 | 1.163 | 1.135 | 1.163 | 0.982 | 1.054 | 1.056 | 1.107 |
| SC15012 | 8.19 | 1.139 | 1.235 | 1.165 | 0.832 | 1.068 | 0.832 | 1.068 | 0.708 | 0.960 | 0.795 | 1.036 |
| SC15015 | 11.40 | 0.911 | 0.996 | 0.947 | 1.036 | 1.148 | 1.036 | 1.148 | 0.868 | 1.018 | 0.960 | 1.089 |
| SC15024 | 21.19 | 0.613 | 0.689 | 0.660 | 1.220 | 1.220 | 1.157 | 1.157 | 0.968 | 0.968 | 1.082 | 1.082 |
| SC20012 | 10.71 | 1.551 | 1.685 | 1.551 | 0.645 | 1.024 | 0.645 | 1.024 | 0.547 | 0.921 | 0.645 | 1.024 |
| SC20015 | 16.48 | 1.215 | 1.327 | 1.240 | 0.890 | 1.194 | 0.890 | 1.194 | 0.746 | 1.063 | 0.855 | 1.162 |
| SC20024 | 33.82 | 0.784 | 0.877 | 0.831 | 1.195 | 1.203 | 1.195 | 1.203 | 0.956 | 1.032 | 1.063 | 1.110 |
| | | | | | Mean | 1.135 | Mean | 1.127 | Mean | 1.005 | Mean | 1.082 |
| | | | | | STDEV | 0.062 | STDEV | 0.055 | STDEV | 0.044 | STDEV | 0.038 |

Table 3. Local Buckling Tests of Plain C- and SupaCee® Channel Sections

| Section | $M_T$ (kNm) | $\lambda_d = \sqrt{\frac{M_y}{M_{od}}}$ | $\lambda_{dp} = \sqrt{\frac{M_p}{M_{od}}}$ | $\lambda_{dn} = \sqrt{\frac{M_{ny}}{M_{od}}}$ | ***Case A*** | | ***Case B*** | | ***Case C*** | | ***Case D*** | |
|---|---|---|---|---|---|---|---|---|---|---|---|---|
| | | | | | $\frac{M_T}{M_y}$ | $\frac{M_T}{M_{sd}}$ | $\frac{M_T}{M_n}$ | $\frac{M_T}{M_{sd}}$ | $\frac{M_T}{M_p}$ | $\frac{M_T}{M_{sd}}$ | $\frac{M_T}{M_{ny}}$ | $\frac{M_T}{M_{sd}}$ |
| C15015w | 9.47 | 1.213 | 1.300 | 1.228 | 0.804 | 1.192 | 0.804 | 1.192 | 0.701 | 1.097 | 0.785 | 1.175 |
| C15019w | 12.94 | 1.065 | 1.141 | 1.085 | 0.888 | 1.192 | 0.888 | 1.192 | 0.774 | 1.093 | 0.855 | 1.163 |
| C15024w | 17.76 | 0.801 | 0.860 | 0.828 | 1.080 | 1.192 | 1.080 | 1.192 | 0.935 | 1.081 | 1.010 | 1.138 |
| C20015w | 12.20 | 1.444 | 1.552 | 1.444 | 0.672 | 1.145 | 0.672 | 1.145 | 0.582 | 1.053 | 0.672 | 1.145 |
| C20019w | 18.85 | 1.250 | 1.342 | 1.263 | 0.821 | 1.245 | 0.821 | 1.245 | 0.712 | 1.143 | 0.804 | 1.230 |
| C20024w | 27.88 | 0.974 | 1.047 | 0.999 | 1.012 | 1.273 | 1.012 | 1.273 | 0.874 | 1.159 | 0.962 | 1.232 |
| SC15012 | 6.56 | 1.217 | 1.319 | 1.226 | 0.662 | 0.983 | 0.662 | 0.983 | 0.563 | 0.892 | 0.651 | 0.973 |
| SC15015 | 10.10 | 1.006 | 1.100 | 1.029 | 0.903 | 1.162 | 0.903 | 1.162 | 0.755 | 1.038 | 0.862 | 1.128 |
| SC15024 | 18.84 | 0.784 | 0.881 | 0.824 | 1.082 | 1.179 | 1.082 | 1.179 | 0.857 | 1.006 | 0.981 | 1.102 |
| SC20012 | 9.27 | 1.458 | 1.585 | 1.458 | 0.557 | 0.956 | 0.557 | 0.956 | 0.471 | 0.867 | 0.557 | 0.956 |
| SC20015 | 13.70 | 1.212 | 1.324 | 1.222 | 0.741 | 1.098 | 0.741 | 1.098 | 0.621 | 0.986 | 0.729 | 1.086 |
| SC20024 | 29.15 | 0.885 | 0.990 | 0.920 | 1.023 | 1.205 | 1.023 | 1.205 | 0.819 | 1.042 | 0.948 | 1.146 |
| | | | | | Mean | 1.152 | Mean | 1.152 | Mean | 1.038 | Mean | 1.123 |
| | | | | | STDEV | 0.096 | STDEV | 0.096 | STDEV | 0.090 | STDEV | 0.086 |

Table 4. Distortional Buckling Tests of Plain C- and SupaCee® Channel Sections

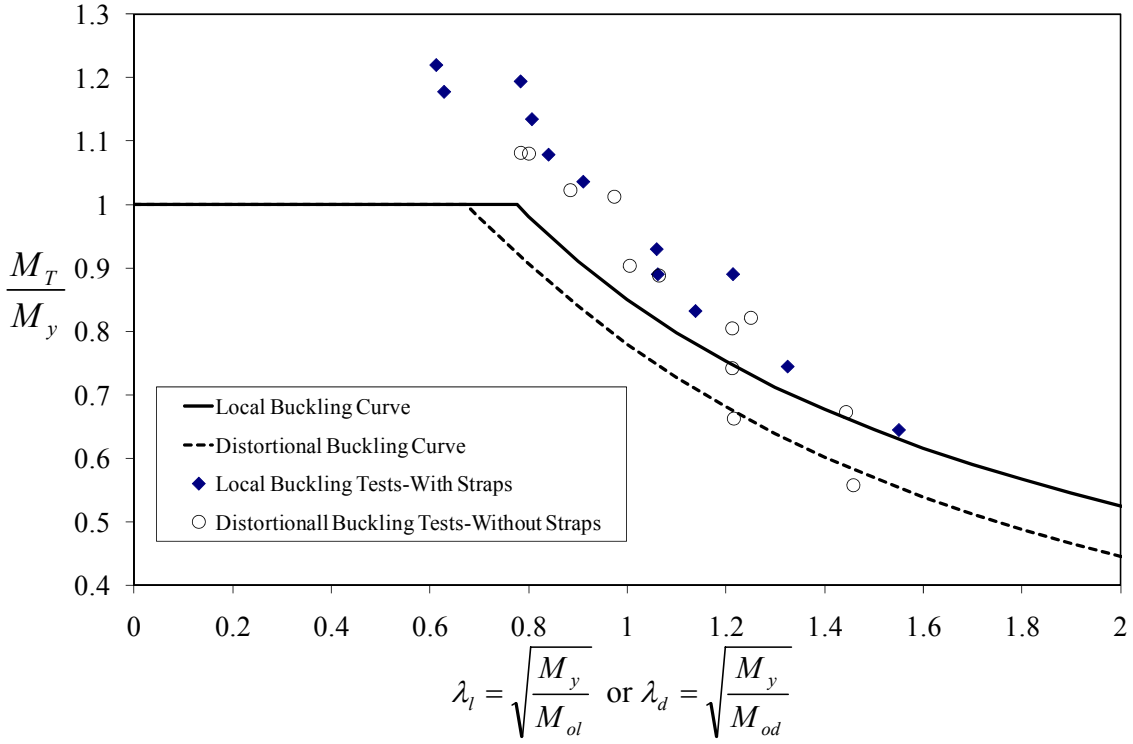


*(a) Case A*

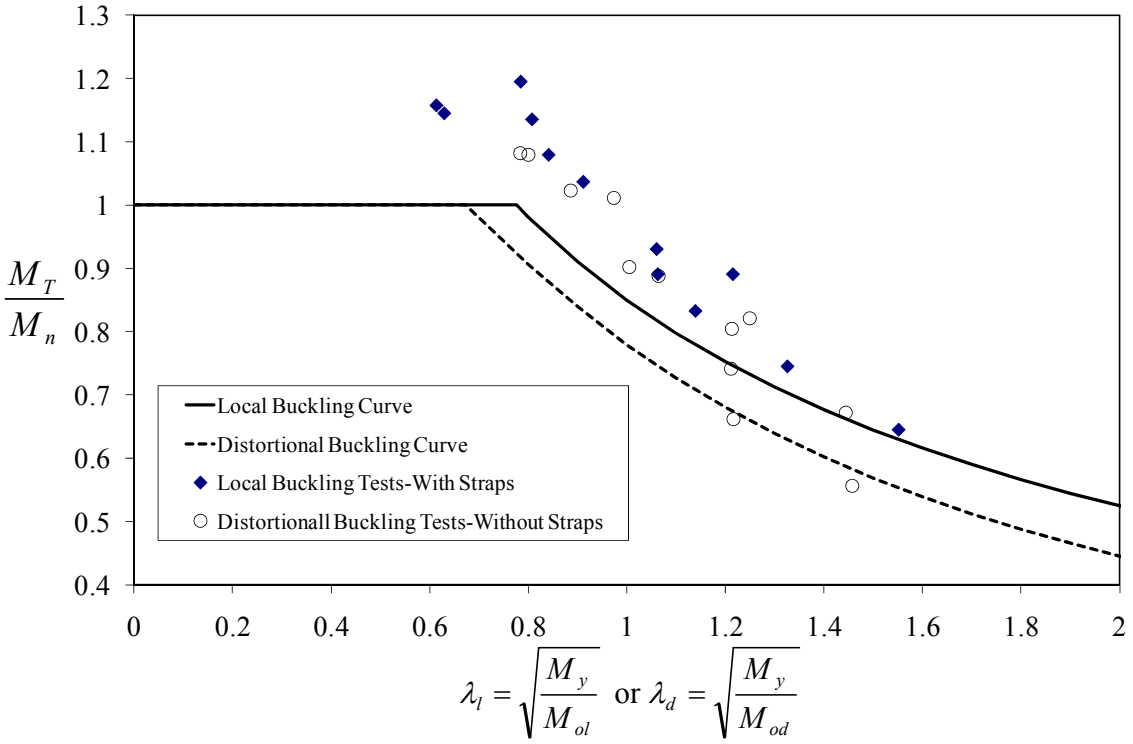


*(b) Case B*

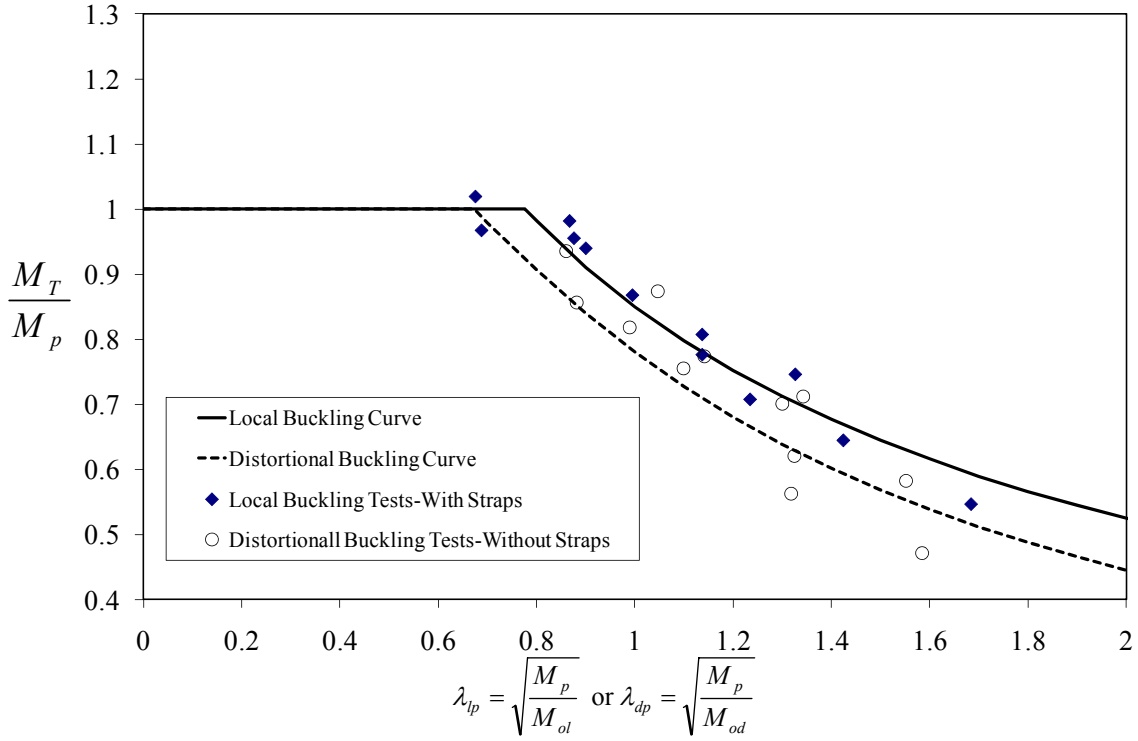


*(c) Case C*

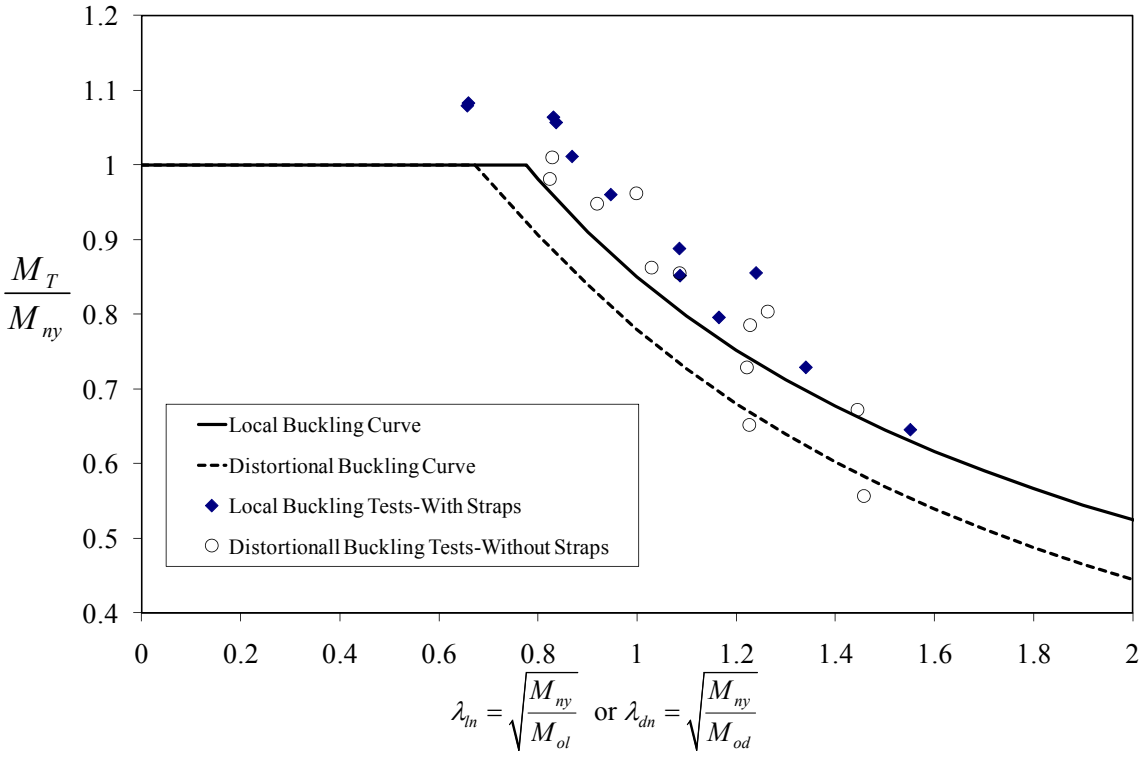


*(d) Case D*

Figure 9. Comparison of the DSM Predictor Curves with Tests Data for Beam- *Cases A, B, C* and *D*

In ***Case A***, the yield moment *($M_y$)* is used in both horizontal axis for non-dimensional slenderness a ($\lambda_l = \sqrt{M_y / M_{ol}}$ and $\lambda_d = \sqrt{M_y / M_{od}}$) and vertical axis for test to predicted capacities *($M_T/M_y$)* as defined in existing DSM rules (Eqs. 1-4). In ***Case B***, while the non-dimensional slenderness is unchanged in the horizontal axis, the yield moment ($M_y$) in vertical axis is replaced by the inelastic bending moment *($M_n$)* as given by Eq. (5) to take into account the effect of inelastic reserve capacity. For ***Case C***, the yield moment *($M_y$)* is replaced by the plastic moment *($M_p$)* in both axes so that $\lambda_{lp} = \sqrt{M_p / M_{ol}}$ and $\lambda_{dp} = \sqrt{M_p / M_{od}}$ as plastic slendernesses. All calculations have been based on the mean measured dimensions and the test values of yield stress *($f_y$)* as shown in Tables 1 and 2 to provide a true measure of design model accuracy.

For the local buckling tests, it can be seen in Table 3 that the means of test results divided by the DSM design local buckling predicted capacities are conservative (1.135 and 1.127) for both ***Case A*** and ***Case B***. The corresponding coefficients of variations are 0.062 and 0.055 respectively. The reason for the slightly different results from ***Case A*** and ***Case B*** is due to the two stocky section tests (C15024 and SC15024) which have the non-dimensional slenderness ($\lambda_l = \sqrt{M_y / M_{od}}$) in the inelastic local buckling reserve range ($\lambda_l \le 0.776$) so that Eq. (5) can be used. For ***Case C***, the results are better predicted (the mean = 1.005) by using $M_p$ instead of $M_y$. The standard deviation for this case is quite low at 0.044.

For the distortional buckling tests, Table 4 shows the same means of test results divided by the DSM design distortional buckling predicted capacities of 1.152 for both ***Case A*** and ***Case B***. This is due to the fact that no sections have the non-dimensional slenderness ($\lambda_d = \sqrt{M_y / M_{od}}$) in the inelastic distortional buckling reserve range ($\lambda_d \le 0.673$). In ***Case C***, the DSM also provides better strength predictions for the distortional buckling failures (the mean=1.038) when $M_p$ is replaced by $M_y$ in comparison with that of ***Case A*** and ***Case B*** (the mean=1.152). The corresponding standard deviation for ***Case C*** is reasonably low at 0.090 compared with 0.096 for both ***Case A*** and ***Case B***.

The prediction of the inelastic local and distortional reserve capacities for cold-formed members was considered in Eq. 5 for ***Case B***. These rules only applied for stocky sections with the slenderness limit of $\lambda_l \le 0.776$ for the inelastic local buckling and $\lambda_d \le 0.673$ for the inelastic distortional buckling respectively. From the tests results shown in Fig. 9(b), for the sections with the non-dimensional slenderness just slightly more slender than the limits for both inelastic local and distortional buckling strength, the test results lie significantly above the two DSM local and distortional design curves when using the yield moment *($M_y$)* in ***Case B***. These sections still have inelastic strength and can develop the plastic moment. As can also be seen in Fig. 9(b), when the sections are more slender, the test results tend to lie closer to the two DSM local and distortional curves. This can be explained by the fact that the more slender are the sections, the less inelastic local and distortional buckling strength they can develop. For very slender sections e.g, SC15012 and SC20012, the loads increased linearly relative to the vertical displacements and the sections buckled in the elastic local and distortional buckling modes.

The alternative ***Case C*** replaces the yield moment *($M_y$)* by the plastic moment *($M_p$)* for both the DSM local and distortional buckling design curves as shown in Fig. 9(c). Although the test results show better strength predictions in comparison with both the DSM local and distortional strength curves, by using $M_p$, the entire test results are shifted down closer to the DSM design curves irrespective of the slenderness. In particular, the test results of the very slender sections (e.g, SC15012 and SC20012) lie considerably lower than both the DSM local and distortional design curves. Therefore, the use of $M_p$ for the very slender sections is unconservative as the sections failed due to the elastic local and distortional buckling prior to developing the plastic moment.

## PROPOSAL FOR DSM EXTENDED INELASTIC STRENGTH IN PURE BENDING

As discussed above, in order to take into account the effect of the inelastic reserve capacity not only for very stocky but also for more slender sections, a proposal called ***Case D*** is used on the basis of the inelastic buckling strength in Eq. 5 with extended non-dimensional slenderness limits. The non-dimensional slenderness for local buckling ($\lambda_l = \sqrt{M_y / M_{ol}}$ =1.55) and for distortional buckling ($\lambda_d = \sqrt{M_y / M_{od}}$ =1.45) is chosen based on those of the most slender section SC20012 for both the local and distortional tests.

The inelastic local and distortional buckling strength is proposed for ***Case D*** as follows:

For $\lambda_l \leq 1.55$ and $\lambda_d \leq 1.45$, and sections symmetric about the axis of bending:

$$M_{ny} = M_y + \left(1 - 1/C_y^2\right)\left(M_P - M_y\right) \tag{6}$$

where $C_{yl} = \sqrt{1.55/\lambda_l} \leq 3$, $C_{yd} = \sqrt{1.45/\lambda_d} \leq 3$, $M_y$ is yield moment, $M_p$ is plastic moment equal to $S_f f_y$ where $S_f$ is the plastic section modulus of the full section and $M_{ny}$ is inelastic moment with extended slenderness limit.

The inelastic non-dimensional slenderness is back-calculated for both local and distortional buckling respectively as $\lambda_{ln} = \sqrt{M_{ny}/M_{ol}}$ and $\lambda_{dn} = \sqrt{M_{ny}/M_{od}}$ which is used along with inelastic moment *($M_{ny}$)* in both axes as shown in Fig. 9d. The test results for ***Case D*** are also summarised in Tables 3 and 4 for local and distortional buckling tests. The means of test results divided by the DSM design local and distortional buckling predicted capacities are 1.082 and 1.123 which are more conservative than those of ***Case C*** but well predicted in comparison with those of ***Case A*** and ***Case B***. It is interesting to note that the corresponding standard deviations for ***Case D*** are 0.038 and 0.086 for the local and distortional buckling tests respectively which are the lowest of all cases.

## CALIBRATION

### RELIABILITY ANALYSIS

The reliability or safety index $\beta_0$ is a relative measure of the reliability or safety of a structure or structural element. When two designs are compared, the one with the larger $\beta_0$ is the more reliable. The reliability index accounts for the uncertainties and variabilities inherent in the design parameters, such as the material properties, geometry, and applied load. In order to calculate the reliability index $\beta_0$, a First Order Second Moment (FOSM) method described by Ellingwood *et al* (1980) can be used. This method is outlined in Chapter F in the North American Specification (AISI, 2007).

The strength of the tested elements, assemblies, connections, or members shall satisfy Eq. F1.1-1a for LRFD from the North American Specification (AISI, 2007) as follows:

$$\sum \gamma_i Q_i \leq \phi R_n \tag{7}$$

where $\sum \gamma_i Q_i$ is required strength [factored loads] based on the most critical load combination determined in accordance with Section A5.1.2 for LRFD. $\gamma_i$ and $Q_i$ are load factors and load effects, respectively. $R_n$ is average value of all test results. The resistance factor $\phi$ is given by:

$$\phi = C_\phi (M_m F_m P_m) e^{-\beta_0 \sqrt{V_M^2 + F_F^2 + C_P V_P^2 + V_Q^2}} \tag{8}$$

where all symbols are defined in Chapter F of the North American Specification (AISI, 2007) and are also included in the Notation. In particular, $P_m$ is the professional factor and gives the accuracy of the model by taking the ratio of the mean value of the tests $R_n$ divided by the model, $F_m$ is the fabrication factor and is the ratio of the actual dimension to nominal dimension, normally thickness as this is the most important dimension for thin-walled sections, and $M_m$ is the material factor which is the ratio of the coupon tests of the material to its nominal value.

The target reliability index $\beta_o$ is taken as 2.5 for cold-formed members. $V_M$, $F_M$ and $V_P$ are the variability of $M_m$, $F_m$ and $P_m$ respectively. $V_Q$ is the variability of the loads taken as 0.21 in the NAS (2007). $C_\phi$ is the calibration coefficient defined as 1.52 in Chapter F of the NAS (2007).

**RESULTS OF RELIABILITY ANALYSES**

The results of the reliability analyses performed using Eq. 8 are given in Table 5 which includes both local and distortional buckling tests on plain C- and SupaCee® channel sections subjected to pure bending. The test results were calibrated for the four different cases (***Case A***, ***Case B***, ***Case C*** and ***Case D***) which are in association with using different yield *($M_y$)*, inelastic *($M_n$)*, plastic *($M_p$)* and extended inelastic *($M_{ny}$)* moments respectively. For all purlin test data, the values of $M_m$, $V_M$, $F_m$ and $V_F$ used throughout are 1.192, 0.031, 1.000 and 0.01 respectively. These values are taken from 1207 tests for steels from 1.0 mm to 3.0 mm over a 12 month period from the mill of Bluescope Steel Limited. The mean professional factor *($P_m$)* is summarized in Table 5. The corresponding coefficients of variations *($V_P$)* are also included in Table 5. The resulting safety indices $\beta_0$ are shown for $\phi$ = 0.9. Alternatively, the resulting $\phi$ values are also shown for a safety index $\beta_0$ of 2.5.

| Moment Case | Local Buckling Tests With Straps | | | | Distortional Buckling Tests Without Straps | | | |
|---|---|---|---|---|---|---|---|---|
| | $P_m$ | $V_P$ | $\beta_0$ ($\phi$=0.9) | $\phi$ ($\beta$=2.5) | $P_m$ | $V_P$ | $\beta_0$ ($\phi$=0.9) | $\phi$ ($\beta$=2.5) |
| *Case A* | 1.135 | 0.055 | 3.728 | 1.181 | 1.152 | 0.083 | 3.606 | 1.165 |
| *Case B* | 1.127 | 0.049 | 3.727 | 1.179 | 1.152 | 0.083 | 3.606 | 1.165 |
| *Case C* | 1.005 | 0.043 | 3.231 | 1.056 | 1.038 | 0.086 | 3.141 | 1.046 |
| *Case D* | 1.082 | 0.035 | 3.599 | 1.141 | 1.123 | 0.076 | 3.547 | 1.145 |

Table 5. Reliability Analyses for Local and Distortional Buckling Tests (Case A,B and C)

For ***Case A*** ($M_y$ is used), the test results are conservatively predicted ($P_m$=1.135 and $V_P$=0.055 for local buckling tests) and ($P_m$=1.152, $V_P$=0.083 for distortional buckling tests) respectively. The corresponding safety index $\beta_0$ and resistance factor $\phi$ of 3.728 and 1.181 for local buckling tests and 3.606 and 1.165 for distortional buckling tests are calibrated respectively. On the basis that a target safety index of 2.5 is required (AISI Commentary 2001 and AS/NZS 4600:1996 Commentary 1998), both local and distortional buckling tests for ***Case A*** have high safety index.

In ***Case B*** ($M_n$ is used), for distortional buckling tests, the safety index $\beta_0$ and resistance factor $\phi$ are identical to those of ***Case A***. The reason for this fact as explained above is that there are no distortional tests without straps whose sections are within the inelastic distortional strength. For local distortional buckling tests, due to the stocky sections (C15024 and SC15024) which have the non-dimensional slenderness in the inelastic local buckling reserve range, the safety index $\beta_0$ and resistance factor $\phi$ slightly reduce to 3.727 and 1.179 for ***Case B*** which are well above the target safety index of 2.5.

With the alternative ***Case C*** ($M_p$ is used), both local and distortional buckling test results are better predicted with respect to $P_m$=1.005 and $V_P$=0.043 (for local buckling) and $P_m$=1.038 and $V_P$=0.086 (for distortional buckling). The corresponding safety index $\beta_0$ and resistance factor $\phi$ are 3.231 and 1.056 for local buckling tests and 3.141 and 1.046 for distortional buckling tests respectively. By comparison with the target safety index of 2.5, the local and distortional buckling tests of both plain C- and SupaCee® channel sections in pure bending have adequate safety indices. However, ***Case C*** includes the very slender cases which are unconservatively predicted when replacing $M_p$ by $M_y$ for all stocky and slender sections.

The safety index $\beta_0$ and resistance factor $\phi$ of proposed ***Case D*** are 3.599 and 1.141 for the local buckling tests and 3.547 and 1.145 for the distortional buckling tests respectively. They are lower than those of ***Case A*** and ***Case B*** but higher than those of ***Case C*** for both the local and distortional buckling tests. The proposed ***Case D*** shows an interesting result of this report that is the use of the inelastic buckling strength $M_{ny}$ for extended slenderness limit range. This proposal allows good predictions to the DSM local and distortional buckling strength for both stocky and slender sections.

## CONCLUSION

An experimental program was carried out to determine the ultimate strength of high strength plain lipped C- and SupaCee® cold-formed channel sections subjected to pure bending. A total of twenty four tests of two different depths and three different thicknesses have been performed at the University of Sydney. While twelve tests were conducted with straps attached evenly in the pure bending region to enforce local buckling

failure, the remaining tests were tested without straps to allow distortional buckling. No tests failed by flexural-torsional buckling due to the lateral bracings. The tests show that, with four small additional multiple longitudinal web stiffeners and return lips as designed on the SupaCee® sections, both buckling and ultimate bending capacities of the complex channel sections have been improved significantly in comparison with those of the plain C- sections. The test results are compared with the DSM prediction equations for both local and distortional buckling in which three different cases associated with yield, inelastic and plastic moments were considered. By comparison, the DSM when using the plastic moment *($M_p$)* instead of the yield moment *($M_y$)* provides good agreement with the results of both local and distortional buckling test series. This alternative produces better correlation with test data and gives more accurate prediction on post-buckling strength of complex channel sections subjected to pure bending. The local and distortional test results are also better predicted by the DSM curves even though the plastic moment *($M_p$)* is used. However, using the plastic moment *($M_p$)* for very slender sections leads to unconservative predictions as the sections failed in elastic local buckling and distortional buckling modes. Therefore, an alternative proposal of this project is that the use of the inelastic moment *($M_{ny}$)*, with extended slenderness limits rather than the plastic moment *($M_p$)* for both DSM local and distortional strength curves, gives good predictions for all stocky and slender sections.

## ACKNOWLEDGEMENT

The authors would like to thank Bluescope Steel for the supply of the test specimens and financial support for the project performed at the University of Sydney. Thanks are also extended to all technicians at the J. W. Roderick Laboratory for Materials and Structures at the University of Sydney. The first author was supported by *GJ Hancock Innovation Fund* and *Centre for Advanced Structural Engineering* scholarships.

## NOTATION

*The following symbols are used in this paper:*

$f_y$ = Yield stress (MPa)
$f_{ol}$ = Elastic local buckling stress of the section in bending (MPa)
$f_{od}$ = Elastic distortional buckling stress of the section in bending (MPa)
$M_{sl}$ = Nominal section moment capacity at local buckling (kNm)
$M_{sd}$ = Nominal section moment capacity at distortional buckling (kNm)
$M_{ol}$ = elastic local buckling moment of the section; $M_{ol} = Z_f f_{ol}$ (kNm)
$M_{od}$ = elastic distortional buckling moment of the section; $M_{od} = Z_f f_{od}$ (kNm)
$M_y$ = Moment causing initial yield at the extreme compression fibre of full section (kNm)
$M_n$ = Inelastic moment (kNm)
$M_{ny}$ = Inelastic moment with extended slenderness limits (kNm)
$M_p$ = Plastic moment (kNm)
$Z_f$ = Section modulus about a horizontal axis of the full section ($mm^3$)
$\lambda_l$ = Elastic slenderness for local buckling $\lambda_l = \sqrt{M_y / M_{ol}}$
$\lambda_d$ = Elastic slenderness for distortional buckling $\lambda_d = \sqrt{M_y / M_{od}}$
$\lambda_{ln}$ = Inelastic slenderness for local buckling $\lambda_{ln} = \sqrt{M_{ny} / M_{ol}}$
$\lambda_{dn}$ = Inelastic slenderness for distortional buckling $\lambda_{dn} = \sqrt{M_{ny} / M_{od}}$
$\lambda_{lp}$ = Plastic slenderness for local buckling $\lambda_{lp} = \sqrt{M_p / M_{ol}}$
$\lambda_{dp}$ = Plastic slenderness for distortional buckling $\lambda_{dp} = \sqrt{M_p / M_{od}}$
$\phi$ = Resistance factor
$C_\phi$ = Calibration coefficient, $C_\phi = 1.52$ for LRFD as specified in Chapter F of the NAS (AISI, 2007)
$M_m$ = Mean value of material factor, *M*
$F_m$ = Mean value of fabrication factor, *F*
$P_m$ = Mean value of professional factor, *P*
$e$ = Natural logarithmic base, $e = 2.718$

$\beta_0$ = Target reliability, $\beta_0 = 2.5$ for cold-formed structural members

$V_M$ = Coefficient of variation of material factor

$V_F$ = Coefficient of variation of fabrication factor

$C_P$ = Correction factor, $C_P = (1+1/n)m/(m-2)$ for $n \geq 4$, $C_P = 5.7$ for $n = 3$ where $n$ =number of tests, $m = n-1$: degrees of freedom

$V_P$ = Coefficient of variation of test results

$V_Q$ = Coefficient of variation of load effect, $V_Q = 0.21$ for LRFD and LSD

## REFERENCES

American Iron and Steel Institute (AISI). (1996). "Specification for the Design of Cold-Formed Steel Structural Members." 1996 Edition, Washington DC.

American Iron and Steel Institute (AISI). (2001). "Commentary on the Load and Resistance Factor Design Specification for Cold-Formed Steel Structural Member." Washington DC.

American Iron and Steel Institute (AISI), "North American Specification for the Design of Cold-Formed Steel Structural Members." 2007 Edition, AISI S100-2007, 2007.

CASE. (2006). "THIN-WALL – A Computer Program for Cross-Section Analysis and Finite Strip Buckling Analysis and Direct Strength Design of Thin-Walled Structures." Version 2.1, Centre for Advanced Structural Engineering, School of Civil Engineering, The University of Sydney.

Cheung, Y. K., "Finite Strip Method in Structural Analysis". *Pergamon Press, Inc.*, New York, N.Y, 1976.

Ellingwood, B., Galambos, T. V., MacGregor, J.G and Cornell, C. A. (1980). "Development of a Probability based Load Criterion for American National Standard A58: Building Code Requirements for Minimum Design Loads in Buildings and Others Structures." Proceedings, Fifteenth International Specialty Conference on Cold-Formed Steel Structures, St Louis, Missouri, U.S.A.

Javaroni, C. E., and Goncalves, R. M., "Distortional Buckling of Simple Lipped Channel in Bending Results of the experimental analysis verses Direct Strength Methods.", *Proceedings, eighteenth International Specialty Conference on Cold-Formed Steel Structures*, 2006,pp. 133-146.

Lysaght., "NSW SupaCee® is trademark of Bluescope Steel Limited." *Bluescope Steel Limited trading as Bluescope Lysaght*, 2003.

Pham, C. H., and Hancock, G. J., "Experimental Investigation of High Strength Cold-Formed C-Section in Combined Bending and Shear.", *Research Report No R894*, School of Civil Engineering, The University of Sydney, NSW, Australia, April, 2009a.

Pham, C. H., and Hancock, G. J., "Experimental Investigation of High Strength Cold-Formed SupaCee® Sections in Combined Bending and Shear.", *Research Report No R907*, School of Civil Engineering, The University of Sydney, NSW, Australia, December, 2009b.

Schafer, B. W., and Ádány, S. (2006). "Buckling of Cold-Formed Steel Members using CUFSM, Conventional and Constrained finite strip methods." Proceedings, Eighteen International Specialty Conference on Cold-Formed Steel Structures, University of Missouri-Rolla, Orlando, Florida, U.S.A., pp. 39-54.

Shifferaw, Y., and Schafer, B. W., "Inelastic Bending Capacity in Cold-formed Steel Members.", *Structural Stability Research Council - Proceedings of the 2007 Annual Stability Conference*, 2007, pp. 279-300.

Standards Australia. (1991). "Methods for Tensile Testing of Metals." AS/NZS 1391, Standards Australia/ Standards New Zealand.

Standards Australia. (1998). "Steel Structures." AS 4100:1998, Standards Australia/ Standards New Zealand.

Standards Australia, "AS/NZS 4600:2005, Cold-Formed Steel Structures." Standards Australia/ Standards New Zealand, 2005.

Yu, C., and Schafer, B. W., "Distortional Buckling Tests on Cold-Formed Steel Members in Bending.", *Journal of Structural Engineering*, American Society of Civil Engineers, Vol. 132, No 4, 2006,pp. 515-528.

Yu, C., and Schafer, B. W., "Local Buckling Tests on Cold-Formed Steel Beams.", *Journal of Structural Engineering*, American Society of Civil Engineers, Vol.129, No12, 2003, pp.1596-1606.

# APPENDICES

| Specimen | b (mm) | A ($mm^2$) | $f_{y0.2\%}$ (MPa) |
|---|---|---|---|
| C15015-1 | 12.33 | 18.50 | 540.58 |
| C15015-2 | 12.45 | 18.68 | 536.46 |
| C15015-3 | 12.34 | 18.51 | 546.36 |
| | | **Mean** | **541.13** |
| C15019-1 | 12.34 | 23.45 | 532.74 |
| C15019-2 | 12.34 | 23.45 | 535.53 |
| C15019-3 | 12.25 | 23.28 | 535.18 |
| | | **Mean** | **534.48** |
| C15024-1 | 12.36 | 29.66 | 491.99 |
| C15024-2 | 12.34 | 29.62 | 478.73 |
| C15024-3 | 12.36 | 29.66 | 485.14 |
| | | **Mean** | **485.29** |
| C20015-1 | 12.42 | 18.63 | 512.12 |
| C20015-2 | 12.43 | 18.65 | 509.12 |
| C20015-3 | 12.43 | 18.65 | 518.97 |
| | | **Mean** | **513.40** |
| C20019-1 | 12.42 | 23.60 | 506.84 |
| C20019-2 | 12.40 | 23.56 | 513.61 |
| C20019-3 | 12.40 | 23.56 | 510.99 |
| | | **Mean** | **510.48** |
| C20024-1 | 12.43 | 29.83 | 479.03 |
| C20024-2 | 12.43 | 29.83 | 489.47 |
| C20024-3 | 12.45 | 29.88 | 481.97 |
| | | **Mean** | **483.49** |

Appendix 1. Coupon Test Results of Plain C-Sections

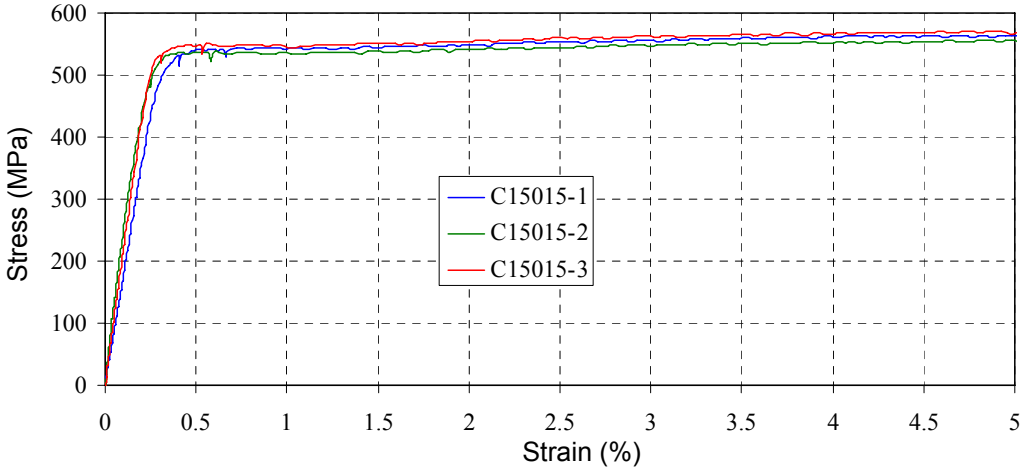


Appendix1-1. C15015 Coupon Tests

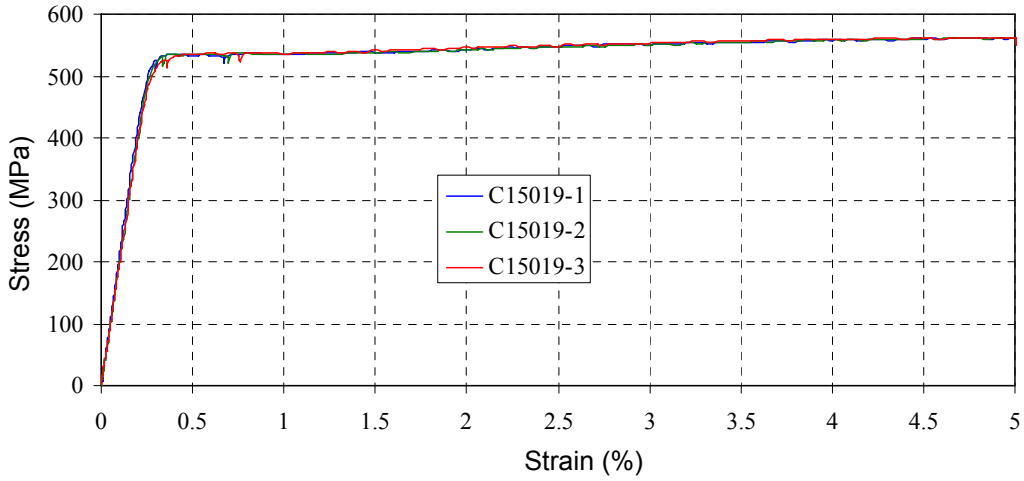


Appendix 1-2. C15019 Coupon Tests

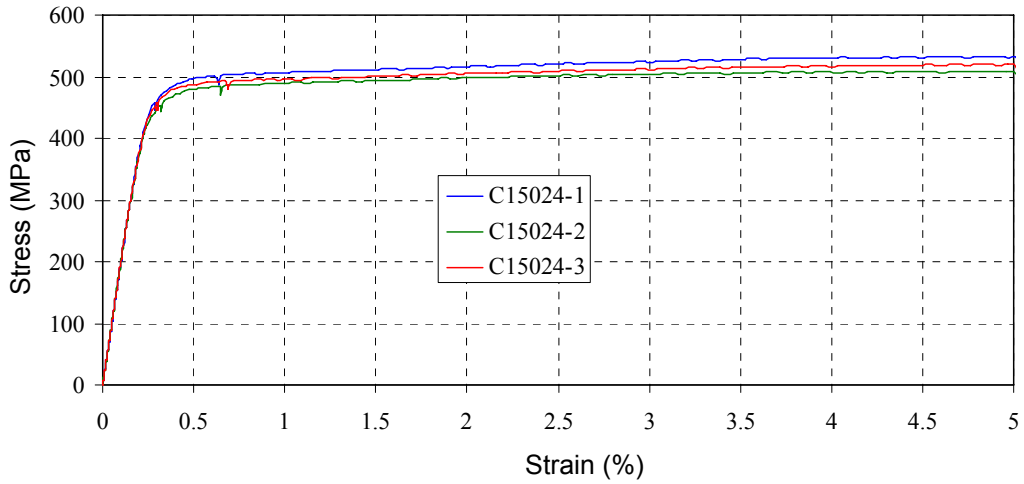


Appendix 1-3. C15024 Coupon Tests

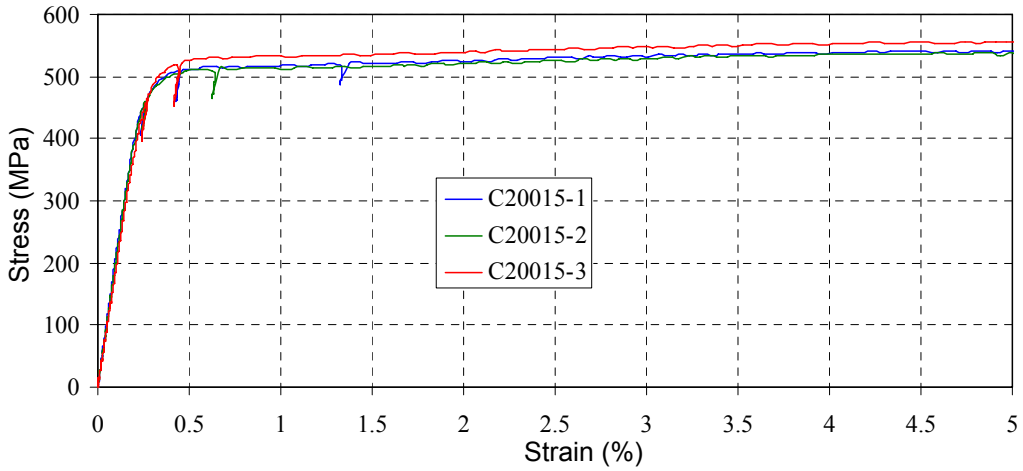


Appendix 1-4. C20015 Coupon Tests

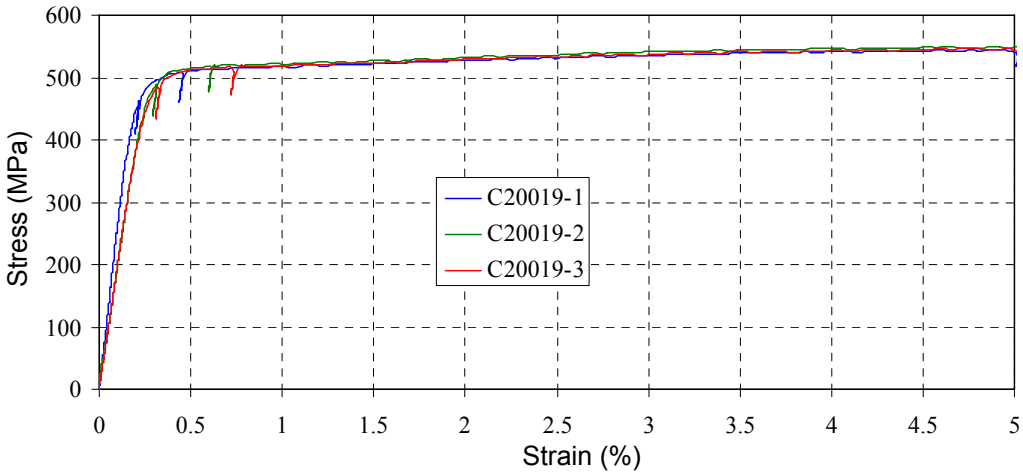


Appendix 1-5. C20019 Coupon Tests

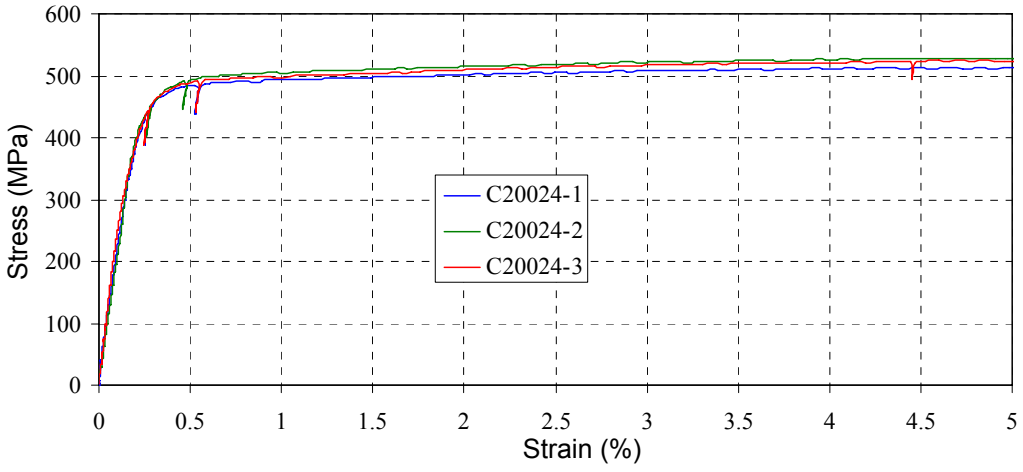


Appendix 1-6. C20024 Coupon Tests

| Specimen | b (mm) | A ($mm^2$) | $f_{y0.2\%}$ (MPa) |
|---|---|---|---|
| SC15012-1 | 12.38 | 14.86 | 590.82 |
| SC15012-2 | 12.34 | 14.81 | 588.31 |
| SC15012-3 | 12.39 | 14.87 | 589.99 |
| | | **Mean** | **589.71** |
| SC15015-1 | 12.41 | 18.62 | 533.18 |
| SC15015-2 | 12.40 | 18.60 | 531.53 |
| SC15015-3 | 12.38 | 18.57 | 536.95 |
| | | **Mean** | **533.88** |
| SC15024-1 | 12.42 | 29.81 | 511.81 |
| SC15024-2 | 12.45 | 29.88 | 517.09 |
| SC15024-3 | 12.44 | 29.86 | 512.13 |
| | | **Mean** | **513.68** |
| SC20012-1 | 12.31 | 14.77 | 595.07 |
| SC20012-2 | 12.31 | 14.77 | 593.00 |
| SC20012-3 | 12.31 | 14.77 | 591.82 |
| | | **Mean** | **593.30** |
| SC20015-1 | 12.21 | 18.32 | 532.17 |
| SC20015-2 | 12.19 | 18.29 | 529.45 |
| SC20015-3 | 12.19 | 18.29 | 534.46 |
| | | **Mean** | **532.03** |
| SC20024-1 | 12.47 | 29.93 | 504.56 |
| SC20024-2 | 12.31 | 29.54 | 505.58 |
| SC20024-3 | 12.41 | 29.78 | 504.83 |
| | | **Mean** | **504.99** |

Appendix 2. Coupon Test Results of SupaCee® Sections

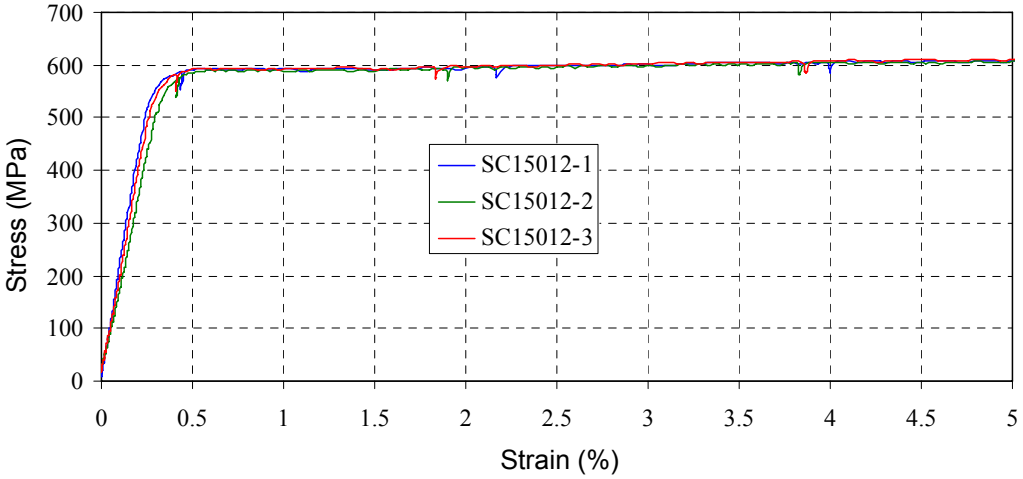


Appendix 2-1. SC15012 Coupon Tests

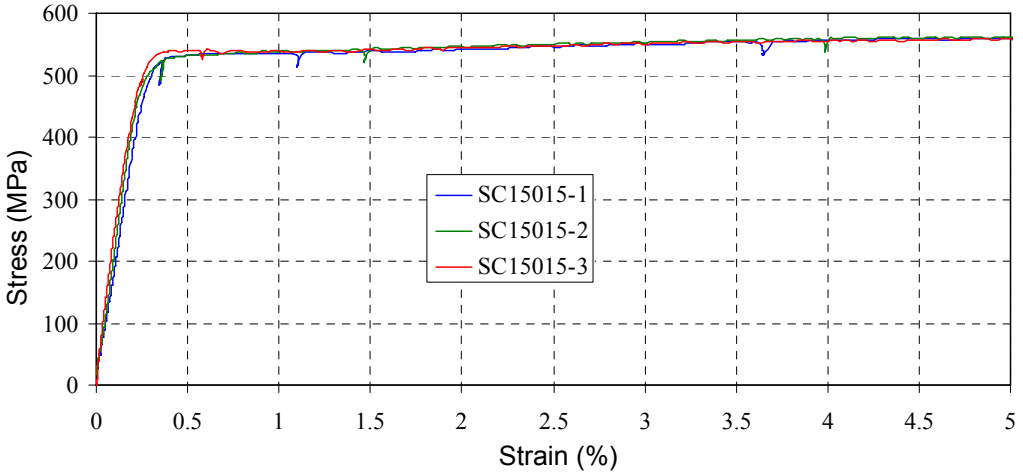


Appendix 2-2. SC15015 Coupon Tests

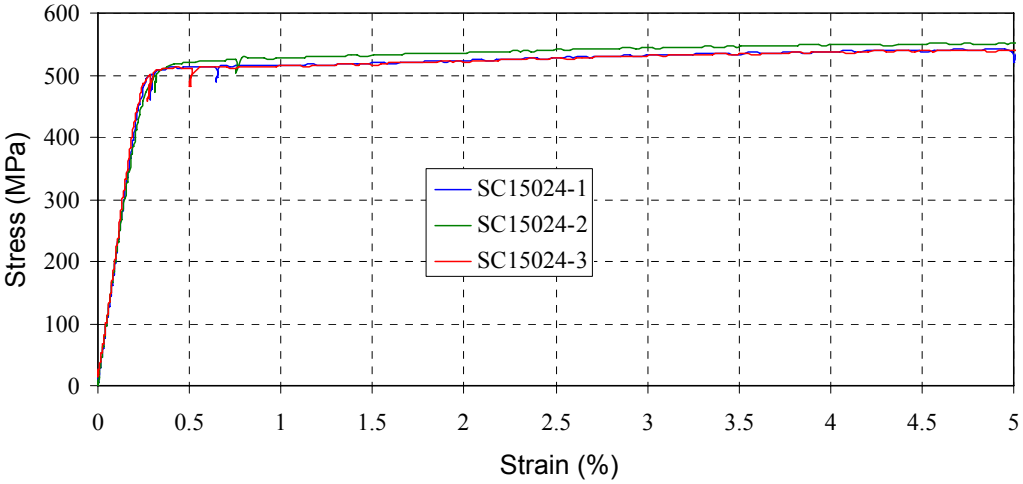


Appendix 2-3. SC15024 Coupon Tests

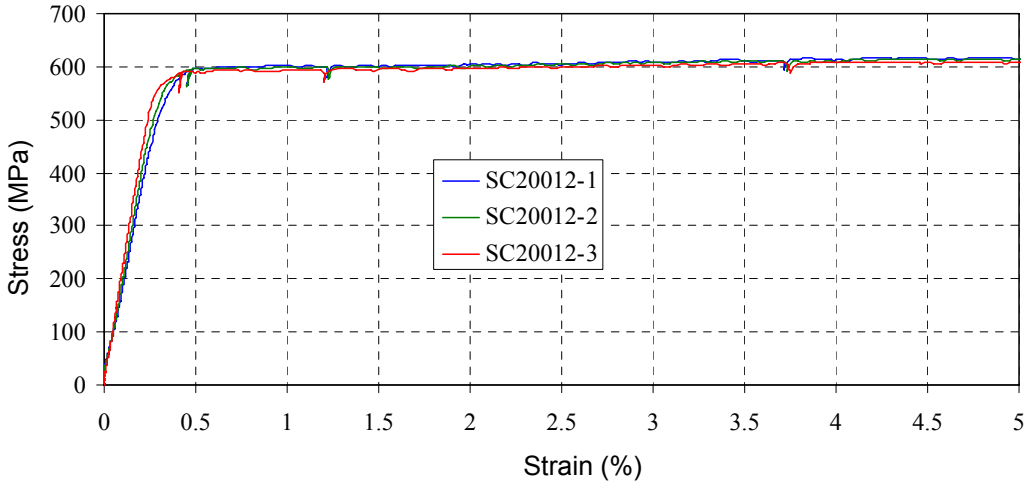


Appendix 2-4. SC20012 Coupon Tests

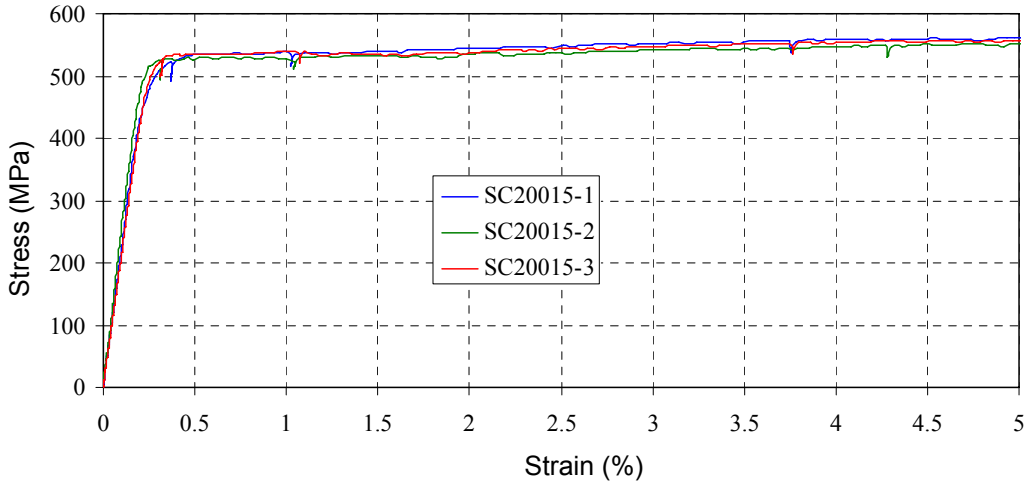


Appendix 2-5. SC20015 Coupon Tests

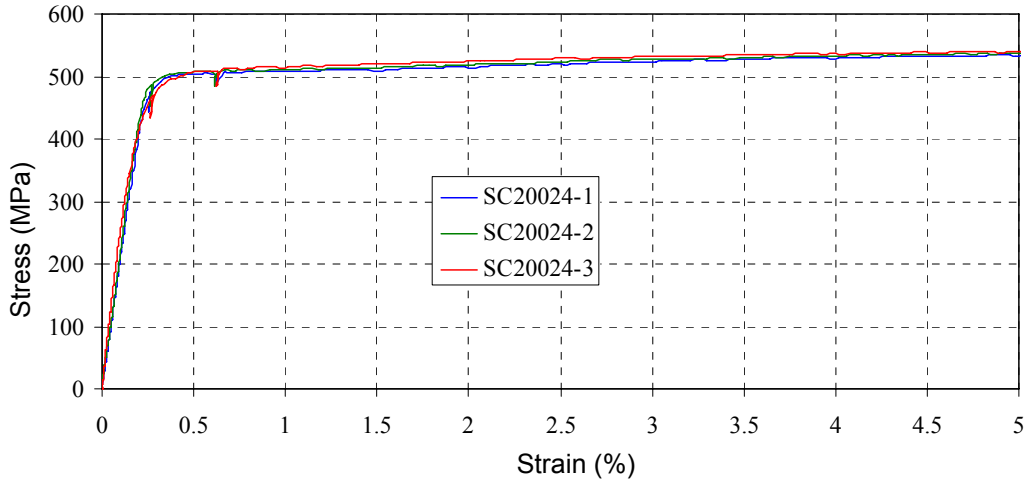


Appendix 2-6. SC20024 Coupon Tests